The Orientation Parameter for Energy Transfer in Restricted Geometries Including Block Copolymer Interfaces: A Monte Carlo Study

Jian Yang and Mitchell A. Winnik*

Department of Chemistry, University of Toronto, 80 St. George Street, Toronto, Ontario M5S 3H6, Canada

Received: June 14, 2005; In Final Form: July 25, 2005

We describe Monte Carlo simulations of resonance energy transfer (RET) experiments for immobile donor (D) and acceptor (A) dyes confined to planar, cylindrical, and spherical restricted geometries. We compare values of the quantum efficiency (Φ_{ET}) evaluated through consideration of individual donor−acceptor pairs, with values calculated assuming a pre-averaged value of the orientation parameter $\langle|\kappa|\rangle^2 = 0.476$ appropriate for infinite three dimensional (3D) space. For dyes confined to restricted geometries where the length scale of the confining dimension is less than or equal to the Förster radius R_0, the coupling of the orientation parameter and the donor−acceptor distance becomes noticeable. Values of Φ_{ET} obtained by proper consideration of the orientation parameter are smaller than those calculated using $\langle|\kappa|\rangle^2 = 0.476$. We use this Monte Carlo method to reanalyze the fluoresce decay measured from dye-labeled poly(isoprene-*b*-methyl methacrylate) diblock copolymer with lamellar structure,[1] from which the interface thickness for PI−PMMA lamella can be retrieved. We found the retrieved interface thickness is sensitive to the choice of dipole orientation. If all dipoles in the confined polymer interface have a random orientation, the value of interface thickness was found to be 0.9 ± 0.2 nm through consideration of individual dipole orientations. Assumption of $\langle|\kappa|\rangle^2 = 0.476$ in the FRET calculations leads to a larger value of interface thickness (1.3 ± 0.2 nm) due to the neglect of the coupling between dipole orientation and D−A distance for the dyes confined to lamellar interfaces.

Introduction

Experiments involving fluorescence resonance energy transfer (FRET) from an electronically excited donor chromophore D to an acceptor chromophore A are very powerful at probing distances on the nanometer scale in biological and synthetic polymer systems.[2] The power of this methodology originates from the strong distance dependence of the energy transfer rate $w(r)$, which for a pair of chromophores, varies with $(R_0/r)^6$, where r is the distance separating the centers of the transition dipoles of the chromophores, and R_0 is the characteristic (Förster) energy transfer distance.[3] It also depends on an orientation parameter κ^2 describing the relative orientation of the two transition dipoles. In biological systems, FRET experiments can be used to determine distances between donors and acceptors, for example, attached to specific sites on a protein or other structure. Often, one is interested in the distribution of distances between the donor and acceptor, which serve as markers for the sites to which they are attached. This type of information is also available through FRET experiments. A characteristic typical of FRET applications to biological systems is that one investigates energy transfer between a single donor and a single acceptor in each molecule. With the sole exception of single-molecule experiments, these measurements sample an ensemble average over many identical molecules.

To interpret the data from a FRET experiment, it is normally necessary to assume that one can use a pre-averaged value of the orientation parameter, whose value can be introduced into the data analysis. This assumption is excellent in the case where the chromophores undergo rotation on a time scale faster than energy transfer. Under these circumstances, $\kappa^2 = \langle\kappa^2\rangle = {}^2/_3$. For the case of an ensemble of molecules, each containing an immobile donor and acceptor, Wu and Brand[4] have shown through simulations that this assumption breaks down. For D−A separations smaller than R_0, the orientation and distance dependences are strongly coupled, and there are many orientations in the random but static configuration where little energy transfer occurs. They point out that this is due to the dipole nature of the dipolar interaction. When two chromophores are far away, the mutual orientation is not as important as when they are close.

In synthetic polymer systems, FRET experiments are particularly useful for studying structure in systems in which the chromophores are confined within a restricted geometry.[5−9] A restricted geometry is defined as domain in which at least one of the characteristic dimensions is on the order of the energy transfer distance for the chromophore pair of interest. R_0 values range from 1 to about 9 nm, and FRET experiments are useful for investigating microdomains with sizes up to several times R_0. The reason that these experiments provide information about structure is that donors near or at the boundary of the domain see a different distribution of acceptors than those in the interior. The nature of this distribution will depend on the shape of the confining structure. For domain sizes much larger than R_0, the number of donors near the edge of the domain represents a negligible fraction of those sampled in a FRET experiment. An important difference between FRET experiments of this sort and those described above for biological systems is that each donor can, in principle, communicate with different acceptors. The FRET kinetics in these systems represents an ensemble average determined by a double integration. For each donor, the experiment integrates over the distribution of nearby

* Author to whom correspondence should be addressed. E-mail: mwinnik@chem.utoronto.ca.

10.1021/jp053204g CCC: $30.25
Published on Web 09/14/2005

CHART 1

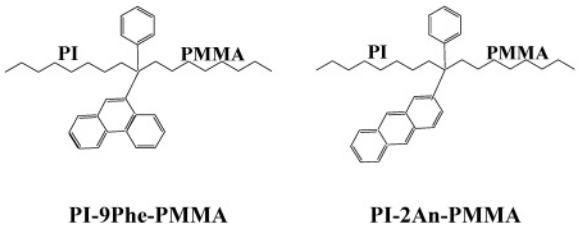

PI-9Phe-PMMA **PI-2An-PMMA**

acceptors. One observes the integrated contribution of all of the donors in the system.

We have been interested in the use of FRET experiments to determine the thickness of the interface between the two different polymers in the periodic microphase-separated domains formed by block copolymers in the bulk state.[1,10−13] These interfaces are of interest because they are often large compared to the size of a monomer unit, but small compared to the dimensions of the polymer molecules themselves. The theory of polymer interfaces predicts that the width of the interface depends primarily on the magnitude of the thermodynamic (Flory−Huggins) interaction parameter (χ_{FH}) characterizing the two polymers.[14,15] For largely immiscible polymers, for which the product of χ_{FH} and the total chain length N is large, the shape of the microdomains depends on the composition of the block copolymers.[16] Symmetrical block copolymers form lamellar structures in the melt. Asymmetric polymers tend to form a hexagonal phase in which the minor component is present as a regular array of cylinders. The minor component of strongly asymmetric polymers forms spheres, which have a body-centered cubic arrangement.

For lamellar structures, other techniques such as specular neutron reflectivity are able to provide rich information about the width of a diffuse interface, whereas for cylindrical and spherical structures, FRET experiments seem particularly appropriate. One of the limitations of the FRET experiments that have been carried out up to date is that the data analysis has neglected the possible contribution to the data of a coupling of the orientation parameter and the donor−acceptor (D−A) distance. We address this problem by using Monte Carlo calculations to generate model data with which to reinterpret fluorescence decay curves previously reported for the lamellar structures formed by poly(isoprene-*b*-methyl methacrylate) (PI−PMMA) diblock copolymers.[1] The polymers we examined contained a single dye, a donor or acceptor, covalently attached to the junction between the PI and PMMA blocks (Chart 1). These dyes serve as tracers for the junction point of the polymers and, in the bulk state, define the span of the interface. To obtain the results described in our previous publication, we analyzed the FRET data in terms of a model that employed a pre-averaged value of the orientation parameter appropriate for static random dipoles in homogeneous three-dimensional (3D) space. Through these data analysis, we learned that this is a system characterized by a very narrow interface, with a width on the order of 1.0 nm, much smaller than R_0 characterizing the donor and acceptor chromophores (2.3 nm). This is the type of system in which coupling of dipole orientation and distance is expected to be most prominent and where it is most important to test the validity of assuming a pre-averaged value of the orientation parameter in the analysis of experimental data.

Monte Carlo (MC) calculations provide an effective way to examine the consequences of pre-averaging the orientation parameter in analyzing FRET data. Since Snyder and Freire[17,18] reported their Monte Carlo simulations to study FRET in two-dimensional bilayers in the 1980s, various research groups have

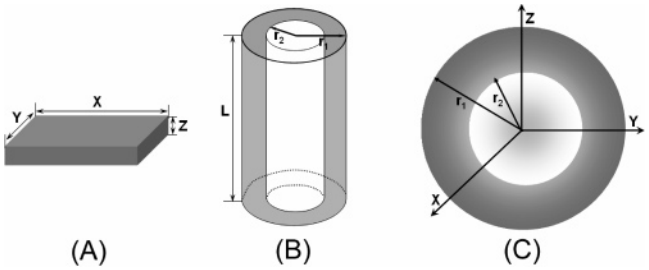

Figure 1. Illustration of the Euclidean-restricted geometries examined: (A) planar slab; (B) cylindrical shell (cylinder when $r_2 = 0$); (C) spherical shell (sphere when $r_2 = 0$).

applied this method to polymer-containing systems with multiple donor−acceptor interactions.[19−21] The most attractive aspect of this method is that one can study FRET by simulating the orientation and distribution of dipoles in many restricted geometries. Wu and Brand[4] used this approach to examine FRET kinetics for the single D−A pair calculations referred to above. We recently reported lattice-based Monte Carlo calculations of FRET kinetics for simulated microphase-separated diblock copolymers with virtual donor and acceptor dyes located at the block junction.[22] We found a coupling effect between the dipole orientation and the D−A distance in the calculation of the efficiency of energy transfer in the simulated lamellar interface. This coupling effect became significant if the interface of the diblock copolymer lamella is narrow and comparable to R_0.

These simulations also provide strong evidence against any significant orientation of the dyes with respect to the plane of the interface. For example, there was very little net orientation of the polymer backbone in the interface. In addition, calculations of FRET kinetics were carried out by assuming that the dipole of the virtual dye in each polymer was aligned with the bond in the polymer backbone connecting the adjacent monomer units. These calculations gave results essentially identical to those obtained by assuming a random dipole orientation for each dye. From this result, we conclude that dyes attached to the junction of block copolymers are well described by a static random dipole orientation in the self-assembled bulk state.

In this paper, we are also interested in the role played by the orientation factor in an energy transfer experiment in which the dyes are confined to a more general Euclidean-restricted geometry. We consider five specific geometries, a thin planar slab, a thin cylinder, a similar cylinder with the dyes confined to a thin cylindrical shell, a small sphere, and a similar sphere in which the dyes are confined to a spherical shell. These systems are depicted in Figure 1. For each of these systems, we assume the donors and acceptors to be uniformly distributed. Most polymer systems are characterized by static but random donor and acceptor pairs. Thus, we will pay less attention to the case where there is a net orientation of the chromophores. For immobile dyes randomly oriented in homogeneous two- (2D) and three-dimensional (3D) space, Baumann and Fayer[23] have shown that FRET kinetics are well described by a pre-averaged orientation parameter $\langle|\kappa^{\Delta/3}|\rangle$, where Δ is the dimensionality. From the results described above, one anticipates that when the chromophores are confined to domains with a characteristic length scale smaller than R_0, the coupling between orientation and distance will become important. Our goal in carrying out Monte Carlo simulations for simple Euclidean shapes is to assess the magnitude of the effect for D and A groups confined to a restricted geometry, and we test our findings by calculating values of the quantum efficiency of energy transfer Φ_{ET}.

Through the use of Monte Carlo calculations, we learn two important lessons. First, we learn that we can take specific account of the coupling of dipole orientation and distance in the analysis of simulated data that gives a best fit to experimental donor fluorescence decay curves. Neglect of this coupling leads to a value of the interface thickness that is too large. Second, we learn that FRET for dyes confined to domains with a thickness on the order of $R_0/2$ to $R_0/4$ are characterized by an effective pre-averaged orientation factor somewhat smaller than that for homogeneous geometries and that the appropriate value to use in the analysis of FRET data can be inferred from the MC studies of FRET for dyes confined to Euclidean-restricted geometries.

Theoretical Considerations

The rate of energy transfer between an electronically excited donor and a nearby acceptor is given by the expression

$$w(r) = \frac{R_{\mathrm{eff}}{}^6}{\tau_{\mathrm{D}} r^6} = \frac{3}{2}\kappa^2 \frac{R_0{}^6}{\tau_{\mathrm{D}} r^6} \tag{1}$$

where τ_{D} is the unquenched lifetime of the donor, and

$$R_0{}^6 = \frac{2}{3}\frac{9000(\ln 10)\Phi_f}{128\pi^5 N_{\mathrm{AV}} n^4}\frac{\int_0^\infty F_{\mathrm{D}}(\lambda)\epsilon_{\mathrm{A}}(\lambda)\lambda^4\,\mathrm{d}\lambda}{\int_0^\infty F_{\mathrm{D}}(\lambda)\,\mathrm{d}\lambda} = 0.353\Phi_f J/(N_{\mathrm{AV}} n^4) \tag{2}$$

In this expression, Φ_f is the fluorescence quantum yield of the donor, n is the refractive index of the medium, and N_{AV} is Avogadro's number. J is the magnitude of the overlap integral, representing the overlap of the emission spectrum ($F_{\mathrm{D}}(\lambda)$) of the donor with the absorption spectrum ($\epsilon_{\mathrm{A}}(\lambda)$) of the acceptor. R_0 is defined for the case of rapidly rotating dipoles, for which $\langle\kappa^2\rangle = {}^2/_3$. In rigid media and in other systems where the orientation parameter takes a value different than ${}^2/_3$, the appropriate characteristic distance is $R_{\mathrm{eff}} = ({}^3/_2)\,\kappa^2 R_0{}^6$, in which the coefficient ${}^3/_2$ removes the orientation parameter contribution to the value of $R_0{}^6$.

For donor and acceptor ensembles in restricted geometries, the theories of energy transfer assume that donor groups are excited with equal probability independent of their location in the matrix. The donor fluorescence decay profile (for instantaneous excitation) is described by a double integration. For each excited donor, the survival probability is described by integration of $w(r)$ and the distribution of acceptors imposed by the geometry of the system. The donor decay profile itself requires a second integration over the distribution of donors in the system. Block copolymer lamellae with dyes attached to specific sites on the polymer (a chain end, along one block, or at the junction) represent examples of restricted geometries, with donors and acceptors distributed along the z-axis normal to a dividing surface. The donor decay profile $I_{\mathrm{D}}(t)$ for this case can be expressed[8]

$$I_{\mathrm{D}}(t) = I_0 \exp(-t/\tau_{\mathrm{D}}) \int C_{\mathrm{D}}(z) \exp[-g(z,t)]\,\mathrm{d}z \tag{3a}$$

$$g(z,t) = 2\pi \int_o^\infty \langle C_{\mathrm{A}}(r,z)\rangle [1 - \exp(-tw(r))] r\,\mathrm{d}r \tag{3b}$$

$$\langle C_{\mathrm{A}}(r,z)\rangle = N_{\mathrm{AV}} \int_{z-r}^{z+r} C_{\mathrm{A}}(r',z)\,\mathrm{d}r' \tag{3c}$$

where I_0 is the intensity at $t = 0$. $C_{\mathrm{D}}(z)$ and $C_{\mathrm{A}}(r, z)$ describe the donor and acceptor distributions, respectively, across the dividing surface.

The important feature of eq 1 is that, for chromophores separated by a given distance r, $w(r)$ depends on three parameters: τ_{D}, R_0, κ^2. The first two parameters can be determined experimentally, but the orientation term is more problematic. For a given pair of chromophores, the orientation parameter is defined as

$$|\kappa| = |\vec{\mathrm{D}}\cdot\vec{\mathrm{A}} - \frac{3}{|\vec{\mathrm{r}}|^2}(\vec{\mathrm{D}}\cdot\vec{\mathrm{r}})(\vec{\mathrm{A}}\cdot\vec{\mathrm{r}})| \tag{4}$$

where $\vec{D}$ and $\vec{A}$ represent unit vectors along the transition dipoles of the donor and acceptor, respectively. In systems with donor and acceptor ensembles, the orientation term embedded in $w(r)$ (eq 3b) has to be considered independently for individual D−A pairs in the calculation of $I(t)$. Only in the case of rapidly reorienting dipoles can the term $\langle\kappa^2\rangle = {}^2/_3$ be factored outside the integration of the energy transfer between the excited donor and its surrounding acceptors. For rigid media, the orientation term is distinct for each pair of chromophores. Under some circumstances, one can calculate an effective pre-averaged value of the orientation parameter. For example, for static but random dyes in 3D, $\langle|\kappa|\rangle = 0.6901$ and $\langle|\kappa|\rangle^2 = 0.476$.[23]

In the calculation of energy transfer in an ensemble of D−A pairs by the Monte Carlo method, one generates an ensemble of discrete points representing the positions of donors and acceptors. Donor survival probabilities and other properties are calculated by taking the appropriate ensemble averages over the distribution of D and A sites in the system. The efficiency of energy transfer, Φ_{ET}, is given by the expression[17]

$$\Phi_{\mathrm{ET}} = 1 - \frac{Q_{DA}}{Q_{\mathrm{D}}} = 1 - \frac{1}{N_{\mathrm{D}}}\sum_{j=1}^{N_{\mathrm{D}}}[1 + \sum_{k=1}^{N_{\mathrm{A}}}\tau_{\mathrm{D}} w(r_{jk})]^{-1}$$

$$w(r_{jk}) = \frac{3}{2}\frac{1}{\tau_D}\kappa_{jk}{}^2(\Omega)\left(\frac{R_0}{r_{jk}}\right)^6 \tag{5}$$

where $w(r_{jk})$ is the rate of energy transfer between the jth donor and kth acceptor separated by a distance r_{jk}. The average orientation factor can be calculated using

$$\langle\kappa^2\rangle = \frac{1}{N_{\mathrm{p}}}\sum_{j\in\mathrm{donor}}\sum_{k\in\mathrm{acceptor}}\kappa_{jk}{}^2(\Omega)$$

$$\langle|\kappa|\rangle = \frac{1}{N_{\mathrm{p}}}\sum_{j\in\mathrm{donor}}\sum_{k\in\mathrm{acceptor}}|\kappa_{jk}(\Omega)| \tag{6}$$

where N_{p} is the total number of D−A pairs in the system. If one uses a pre-averaged orientation factor, $\langle\kappa^2\rangle$ (or $\langle|\kappa|\rangle^2$), Φ_{ET} can be simplified to

$$\Phi_{\mathrm{ET}} = 1 - \frac{1}{N_{\mathrm{D}}}\sum_{j=1}^{N_{\mathrm{D}}}\left[1 + \frac{3}{2}\langle\kappa^2\rangle\sum_{k=1}^{N_{\mathrm{A}}}\left(\frac{R_0}{r_{jk}}\right)^6\right]^{-1} \tag{7}$$

If one assumes that the concentration of excited donors is sufficiently low, the normalized fluorescence intensity decay, corresponding to instantaneous excitation, can be written as

$$I(t) = \frac{I_0}{N_{\mathrm{D}}}\exp\left(-\frac{t}{\tau_{\mathrm{D}}}\right)\sum_{j=1}^{N_{\mathrm{D}}}\exp\left(-\frac{3}{2}\frac{t}{\tau_{\mathrm{D}}}\sum_{k=1}^{N_{\mathrm{A}}}\kappa_{jk}{}^2(\Omega)\left(\frac{R_0}{r_{jk}}\right)^6\right) \tag{8}$$

Note that, in this expression, for each donor, one sums explicitly over the product of $\kappa^2(\Omega)$ $(R_0/r)^6$ for each acceptor. When the orientation parameter can be pre-averaged, the orientation parameter can be taken outside the summation over acceptors, and the calculation simplifies to

$$I(t) = \frac{I_0}{N_D} \exp\left(-\frac{t}{\tau_D}\right) \sum_{j=1}^{N_D} \exp\left(-\frac{3}{2}\langle\kappa_{jk}{}^2(\Omega)\rangle \frac{t}{\tau_D} \sum_{k=1}^{N_A} \left(\frac{R_0}{r_{jk}}\right)^6\right) \quad (9)$$

Monte Carlo Calculations

We used a Monte Carlo strategy for the random placement of points representing donor and acceptor dyes in confined geometries. One set of simulations involved dyes confined to Euclidean geometries of finite size. We use the term "Euclidean" geometries to refer to planar slabs, cylinders, and cylindrical shells, as well as spherical shells, as depicted in Figure 1. A second set of simulations were intended to generate dye distributions that might be expected for dyes attached to the junction points of diblock copolymers in a microphase-separated lamellar geometry.

Construction of Dye Distributions for Euclidean Geometries. Virtual donors and acceptors were introduced as point objects at random into the volume elements described by the objects shown in Figure 1. Periodic boundary conditions were employed. These extend in the *X* and *Y* directions for the confined planar slab (Figure 1A), and they extend in the *L* direction in cylindrical geometries (Figure 1B). No periodic boundary condition was applied for spherical geometries (Figure 1C). The confined dimension was defined in units of R_0. Periodic boundary conditions were applied whenever an acceptor within $5R_0$ of a donor was located within the extended planar slab or extended cylinder. The orientation factor and quantum efficiency of energy transfer Φ_{ET} were averaged by summing over all donors in the restricted geometry. In a typical calculation, 10 000 donor sites were generated, and the acceptor concentration was kept constant at $2\pi/3$ per sphere of radius R_0. The donor concentration is unrealistically high, but this does not interfere with the simulation. We sample only donor−acceptor interactions, and the large number of donors helps improve counting statistics. Donor−donor interactions play no role in the quantities computed.

To generate the loci of donors and acceptors in a restricted geometry, each coordinate, *x* (or *y*, or *z*), of a dye was given by a random number, generated by computer (DELPHI). This random number fell in the range of the dimension of the restricted geometry along the *X* (or *Y*, or *Z*) axes. For example, in a planar slab, a random number was generated along the *X*-axis in the range from 0 to X_{max} (see below), and its value was set equal to *x*. The remaining coordinates for the dye locus (*y*, *z*) along the *Y* and *Z* axes were generated in a similar way. In a cylindrical shell, the coordinate of a dye in the *L* direction was generated in the same way, but the coordinates of this dye in the plane perpendicular to *L* direction (*x*, *y*) were randomly generated with the restriction of $r_2 \le r\ (= \sqrt{x^2+y^2}) \le r_1$, where r_1 and r_2 are the outer and inner radii of the cylindrical shell ($r_2 = 0$ for a solid cylinder), respectively. In a spherical shell, the coordinates of a dye locus (*x*, *y*, *z*) were randomly generated with the restriction $r_2 \le r\ (= \sqrt{x^2+y^2+z^2}) \le r_1$, where r_1 and r_2 are the outer and inner radii of the spherical shell ($r_2 = 0$ for a solid sphere), respectively.

To generate a random dipole orientation for each dye locus, we chose three random numbers in the range from −0.5 to 0.5. These three random numbers were used as the orientation vectors of a dipole in the *X*- ($\vec{x}$), *Y*- ($\vec{y}$), and *Z*-directions ($\vec{z}$). The unit vector of this dipole orientation $\vec{D}$ (or $\vec{A}$) can be expressed by $\vec{D} = (\vec{x}, \vec{y}, \vec{z})/\sqrt{\vec{x}^2 + \vec{y}^2 + \vec{z}^2}$, where $\sqrt{\vec{x}^2+\vec{y}^2+\vec{z}^2}$ is a normalization factor.

Once the loci and orientation of these virtual dyes were established, we calculated parameters related to energy transfer by a complete summation over all donors and acceptors in the system. To simplify the calculation, for each donor, we summed only over those acceptors for which $r_{jk} < 5R_0$.

TABLE 1: Characteristics of the Diblock Copolymers

polymers	M_n (dye content)[a]	PDI[b]	V_{PI}/V_{PMMA}[c]
PI-9Phe-PMMA	32600 (1.0)	1.17	51.5:48.5
PI-2An-PMMA	28600 (0.93)	1.11	51.2:48.8

blend sample	(f_{Phe})[d]	$C_A{}^0$ (mM)[e]	H[f] (nm)
1	0.50	16.45	26
2	0.73	8.75	26
3	0.86	4.43	26

[a] Fraction of polymer molecules x_{dye}, which contain a dye attached to the junction: donor dye, 9-phenanthryl (Phe), acceptor dye, 2-anthryl (An). [b] Polydispersity M_w/M_n. [c] Volume ratio of PI to PMMA. [d] Calculated from $f_{Phe} = m_{PI-9Phe-PMMA}/(m_{PI-9Phe-PMMA} + x_{An}\, m_{PI-An-PMMA})$, where *m* refers to the number of moles of each component and x_{An} is the fraction of chains bearing An groups for the An-labeled diblock copolymer samples. [e] Calculated from the mole number of An ($m_{PI-An-PMMA}$), the degree of labeling (x_{An}), the mean number-averaged molecular weight of the polymer (M_n), and the polymer density (ρ), $C_A{}^0 = x_{An}\, m_{PI-An-PMMA}/(M_n\, \rho)$. [f] Lamellar spacing inferred from SAXS measurements on the pure components.

Construction of Dye Distributions for the PI−PMMA Lamellar Interface. The lamellar block copolymer microphase was simulated as a single lamellar component whose overall width corresponds to the measured lamellar spacing $H/2 = 13$ nm, determined by small-angle X-ray scattering (SAXS) for the PI−PMMA samples of interest.[1] The characteristics of these polymers are summarized in Table 1. As described in ref 1, the chromophores (donors and acceptors) were labeled at the junctions of PI and PMMA blocks. As a consequence, they are confined to the interface between the PI and PMMA blocks. The spatial distribution of the donor (Phe) and the acceptor (An) across the interface can be represented by the distribution of the block junctions. According to Helfand−Tagami mean field theory,[14,24] the junction distribution density $P_j(Z)$ across the interface is given by

$$P_j(Z) = \frac{2\pi}{\delta} \sec h\left(\frac{2Z}{\delta}\right) \quad (10)$$

where δ is the interface thickness. *Z* (ranging from $-H/4$ to $H/4$) is the coordinate in the direction perpendicular to the interface plane. The center of the interface was located at $Z = 0$. For the dimensions of interface plane, we set $L_X = L_Y = 100$ nm and applied periodic boundary conditions in both directions. The number of acceptors introduced into the $13 \times 100 \times 100$ nm^3 simulation box was chosen to correspond to the mean molar concentration of acceptors in the block copolymer sample. For example, in simulations of sample 2 (cf. Table 1) containing 73% Phe-labeled polymer in the mixture of donor- and acceptor-labeled PI−PMMA, the number density of acceptors corresponded to the experimental value $C_A{}^0 = 8.75$ mM. The bulk concentration of donor was fixed at 5 mM. We considered a series of slices at difference *Z* values. Within each slice, the number density of acceptors was uniform, but in the *Z* direction, the concentration profile was selected to match the junction distribution predicted by eq 10 and shown in Figure 2A. For

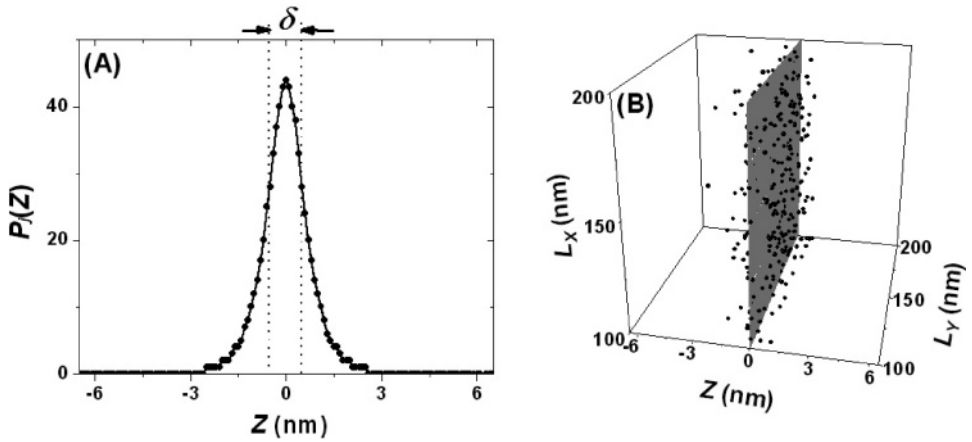

Figure 2. Simulation of one period of a block copolymer lamellar structure with a domain thickness of 13 nm ($H/2$, H is the lamellar spacing) and an interface width of $\delta = 1.0$ nm. (A) Spatial distribution of the junctions $P_j(Z)$ across the interface centered at $Z = 0$. The magnitude of the interface width δ is indicated in the figure. (B) The loci of acceptors ($C_A^0 = 8.75$ mM) corresponding to junctions in the lamellar structure as generated by a Monte Carlo calculation. The gray plane is the center of the interface located at $Z = 0$.

each slice with a certain Z value, we calculated the number of donors and acceptors based on eq 11.

$$N_A(Z) = N_A{}^0 P_j(Z) / \sum_{Z=-H/4}^{H/4} P_j(Z)$$

$$N_A{}^0 = N_{AV} C_A{}^0 L_X L_Y H/2 \qquad (11)$$

where N^0_A are the total number of acceptors in the simulation box. Those acceptors were randomly put into the slice. An example of the acceptor distribution corresponding to $C_A{}^0 = 8.75$ mM is shown in Figure 2B. The donor concentration profile was constructed in a similar manner. In initial simulations, the total number of donors was chosen to match $C_D{}^0$ values for each sample. The results obtained, however, were independent of the number of donors in the simulation box for the range of donor numbers examined, presumably because of the $(1/N_D)$ term in eqs 5, 7, 8, and 9. The results reported here all involve calculations corresponding to $C_D{}^0 = 5$ mM.

Values of the energy transfer quantum efficiency and donor fluorescence decay profiles were evaluated by summing over all donor−acceptor pair combinations in the ensemble for which $r_{jk} < 5R_0$. For both Euclidean-restricted geometries and for the block copolymer lamella, to obtain standard deviations, five separate calculations were carried out on the basis of independent generation of loci for donors and acceptors.

Results and Discussion

We begin with an examination of FRET kinetics in Euclidean-restricted geometries, presenting results in turn for the three general shapes of the confining geometry (planar, cylindrical, and spherical) as shown in Figure 1. For each structure, we examine Φ_{ET} as a function of the confinement in units of R_0. While our focus is on immobile dyes with a random orientation, which is appropriate for most systems involving polymers in the bulk state, we also consider examples of oriented dipoles in which, for comparative purposes, we make extreme and unrealistic assumptions about the orientation of transition dipoles.

Planar Geometry. As shown in Figure 1A, the plane is restricted only in the Z-direction. We set $X_{max} = Y_{max} = 50R_0$ and applied periodic boundary conditions in both directions. Donors and acceptors were randomly located within the planar slab. The confining dimension Z was varied from 0 to $50R_0$. We set the number of donors within the confined geometry to 10 000 per $50R_0 \times 50R_0$ area (4 donors per $R_0 \times R_0$ area). The concentration of acceptors was fixed at $2\pi/3$ per sphere of radius R_0, which in the limit of $Z \rightarrow 0$, corresponds to $2\pi/3$ per circle of radius R_0.

We treat the virtual dyes as points of zero volume, making it possible for a D−A pair to be unrealistically close. To test whether this possibility makes a significant contribution to the extent of energy transfer, we calculated the distance distribution of D−A pairs in the 2D system with $Z = 0$, which has the highest density of donors. These results show that only 0.3% of total D−A pairs are separated by less than $0.3R_0$, and for this system, $\Phi_{ET} = 0.762 \pm 0.005$. If we assumed that all dyes have an excluded circle (in two dimensions) of radius $0.3R_0$, $\Phi_{ET} = 0.764 \pm 0.003$. We conclude that, for the acceptor concentrations employed here, neglecting the volume occupied by the dyes makes no significant contribution to the extent of energy transfer.

Random Dipole Orientation. For disordered dipole orientation of immobile donors and acceptors, Baumann and Fayer found that the system was characterized by a pre-averaged orientation factor independent of the individual dipole orientations. For Euclidean geometries, this term takes the form $\langle|\kappa|^{\Delta/3}\rangle$ where Δ is the Euclidean dimension. We used eq 6 to compute mean values of the orientation parameter. For $Z = 0$, we found $\langle|\kappa|^{2/3}\rangle = 0.741 \pm 0.002$, which compares well to the value 0.7397 calculated by Baumann and Fayer. In 3D, we found that $\langle|\kappa|\rangle$ is almost independent of the confinement scale and close to the value calculated by Baumann and Fayer (0.6901, line (d) in Figure 3).

Values of Φ_{ET} as a function of Z value are presented in the upper part of Figure 3. Curve (c) refers to the data obtained with eq 5, which takes specific account of the orientation of individual dipoles. At large values of Z/R_0, Φ_{ET} approaches the value expected for homogeneous dye distribution in the bulk state, with an acceptor concentration in units of $(4/3\pi R_0{}^3)^{-1}$.[25] For values of $Z/R_0 < 10$, there is a sharp decrease with a decrease in Z. Two factors could, in principle, contribute to this decrease. One contribution is due to the reduction in the number of acceptors around each donor as a consequence of edge effects of the confining space. Another contribution could come from a decrease in the energy transfer probability of nearby D and A groups because of orientation effects. The close similarity between curve (c) in Figure 3 and curve (b), calculated with a pre-averaged orientation factor of $\langle|\kappa|\rangle^2 = (0.6901)^2 = 0.476$,

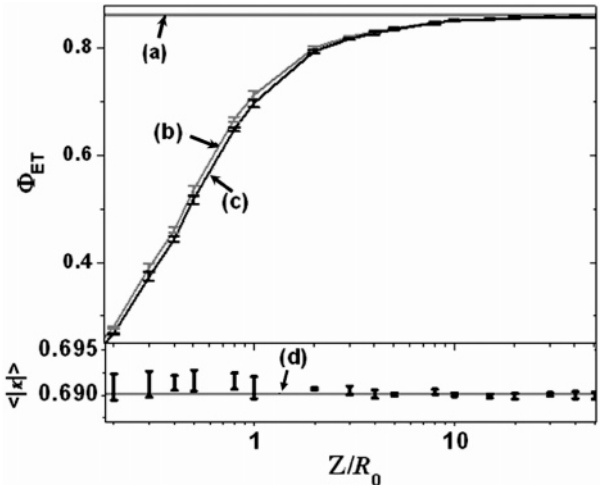

Figure 3. Efficiency of energy transfer Φ_{ET} for donors and acceptors confined to a planar slab as a function of Z/R_0. (a) Value of Φ_{ET} calculated for an infinite 3D system with $\langle|\kappa|\rangle^2 = 0.476$. (b) Values of Φ_{ET} calculated with eq 7, taking the pre-averaged orientation factor value $\langle|\kappa|\rangle^2 = 0.476$. (c) Values of Φ_{ET} calculated with eq 5 for random dipoles, considering the individual orientation for each donor and acceptor pair. The number of donors was set to 10000 (4 donors per $R_0 \times R_0$ area). Acceptor concentration is $2\pi/3$ per sphere of radius R_0. Lower part: values of the averaged orientation factor ($\langle|\kappa|\rangle$ for random dipoles compared with the line (d), representing the Baumann and Fayer[23] value appropriate for infinite 3D space.

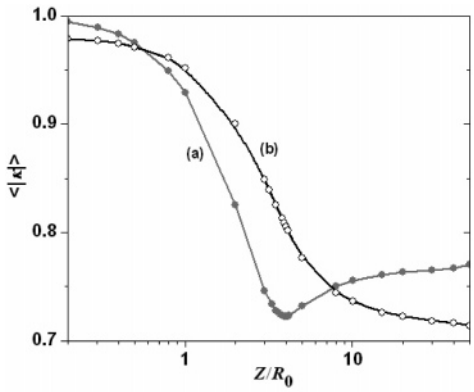

Figure 4. Dependence of the average orientation factor ($\langle|\kappa|\rangle$) on the thickness (Z/R_0) of a planar slab when all dipole orientations are perpendicular (curve a) or parallel (curve b) to the confinement plane. The errors associated with each calculation are within the size of the symbols.

indicates that the quantum efficiency of energy transfer is much more sensitive to confinement effects on the donor and acceptor distribution than to coupling of the orientation term to the donor−acceptor separation, even for these short distances. Φ_{ET} values based on $\langle|\kappa|\rangle^2 = 0.476$ are slightly larger than those calculated from pairwise consideration of dipole orientation. This result, which turns out to be important, indicates that, for $Z/R_0 \leq 1$, FRET kinetics can be described in terms of a pre-averaged orientation factor, with a magnitude somewhat smaller than 0.476.

Oriented Dipoles. When the dipoles in a system are oriented, the extent of energy transfer will be larger than for random dipoles if parallel orientation is enhanced. If perpendicular orientation is enhanced, the net extent of FRET will decrease. In this section, we consider two extreme cases of dipole orientation, dipoles aligned in the Z direction, and dipoles randomly oriented in the X,Y plane. In Figure 4, we plot the mean values of $\langle|\kappa|\rangle$ as a function of Z/R_0 computed for these examples. For dipoles aligned parallel to the X,Y plane, $\langle|\kappa|\rangle$ increases with decreasing values of Z/R_0 and has a limiting value somewhat less than unity at $Z = 0$. Here, for two dimensions, we calculate $\langle|\kappa|^{2/3}\rangle = 0.9458 \pm 0.0006$, which is identical to the value reported by Baumann and Fayer (0.9462).[23] For dipoles aligned along the Z direction, the dependence of $\langle|\kappa|\rangle$ is more complex. It assumes a value of unity at $Z = 0$ (where all the dipoles are parallel), decreases strongly for increasing Z/R_0, passes through a minimum at $Z = 4R_0$, and then increases slowly.

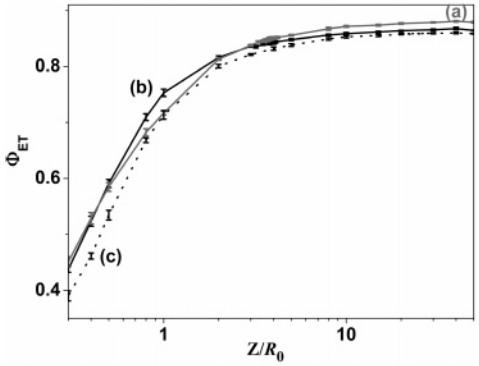

Figure 5. Efficiencies of energy transfer calculated considering the individual orientation for donors and acceptors confined to a planar slab at a fixed acceptor concentration ($2\pi/3$ per $4\pi R_0^3/3$ of volume) as a function of Z/R_0. (a) Dipoles of donors and acceptors were aligned in the Z direction. (b) All dipoles lie parallel to the (X,Y) plane, but randomly oriented within the plane. (c) Φ_{ET} calculated with an averaged orientation factor $\langle|\kappa|\rangle^2 = 0.476$.

Values of Φ_{ET} for these two cases are plotted as a function of Z/R_0 in Figure 5. Here, one sees a stronger sensitivity of Φ_{ET} to dipole orientation than in the case of random dipoles, and both examples lead to higher efficiencies of energy transfer than one would compute assuming a pre-averaged value of $\langle|\kappa|\rangle = 0.6901$. There is an interesting crossover in the data, with dipoles parallel to the Z axis, leading to higher values of Φ_{ET} for $Z > 5R_0$, and dipoles parallel to the X,Y plane, generating higher values of Φ_{ET} for $Z < 5R_0$. We conclude that there is no pre-averaged orientation factor that can properly describe FRET kinetics for either of these cases of oriented dipoles. Nevertheless, the quantitative effect of assuming a pre-averaged value of $\langle|\kappa|\rangle = 0.6901$ is a relatively small underestimation of the extent of energy transfer.

Cylindrical Geometry. As in the case of a rectangular box, we assume a random distribution of D and A, with 10 000 donors within the cylindrical shell and a uniform acceptor concentration of $2\pi/3$ per sphere of radius R_0. In the calculations, L_{max} was set to $50R_0$, and periodic boundary conditions were applied in the L direction. For cylinders, we examine random dipoles as well as the hypothetical case in which all dipoles are oriented in the radial direction.

A cylinder is a special case of a cylindrical shell in which the inner radius r_2 is equal to zero. In Figure 6, we plot the change of Φ_{ET} with the radial dimension (r_1) of the cylinder. The dotted curve (b) calculated, assuming a pre-averaged $\langle|\kappa|\rangle = 0.6901$, tracks very close to values obtained for pairwise consideration of random dipole orientation (curve (c)). When r_1 decreases to a value comparable to R_0, the value Φ_{ET} obtained by assuming $\langle|\kappa|\rangle = 0.6901$ is slightly larger than the value for random dipoles. For example, the difference is 3% at $r_1 = R_0$, and 1% at $r_1 = 2R_0$. For the case of radial dipole orientation, the calculated Φ_{ET} values (curve (a)) are larger than those for random dipoles at large values of r_1. Irrespective of the dipole orientation, the dominant factor that leads to a decrease in Φ_{ET}

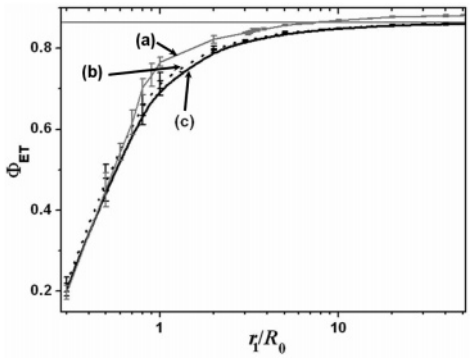

Figure 6. Efficiency of energy transfer Φ_{ET} for donors and acceptors confined to a thin cylinder as a function of the radius r_1/R_0. The donors and acceptors are randomly distributed, and the acceptor concentration is $2\pi/3$ per $4\pi R_0^3/3$ of volume. (a) All dipoles have a radial orientation. (b) Φ_{ET} calculated using a pre-averaged orientation factor $\langle|\kappa|\rangle^2 = 0.476$. (c) Φ_{ET} values calculated by assuming a random dipole orientation for each donor and acceptor. The straight line in the upper part of the figure is the value of Φ_{ET} calculated for a uniform acceptor concentration in extended 3D space assuming $\langle|\kappa|\rangle^2 = 0.476$.

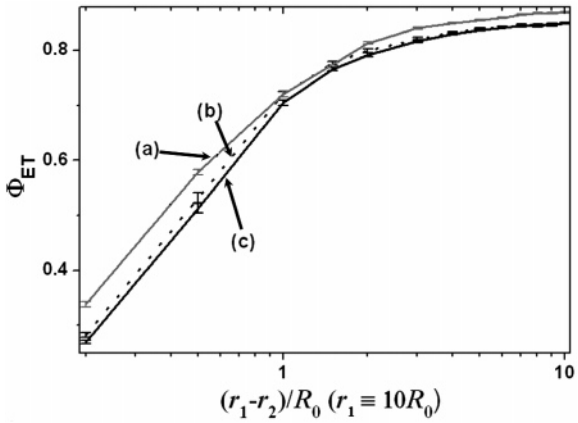

Figure 7. Efficiency of energy transfer Φ_{ET} for randomly distributed donors and acceptors confined to a thin cylindrical shell as a function of the shell thickness $(r_1 - r_2)/R_0$ for a fixed outer radius ($r_1 = 10R_0$). The acceptor concentration is $2\pi/3$ per $4\pi R_0^3/3$ of volume. The solid lines are the Φ_{ET} values calculated by considering individual orientation factors for each D−A pair with the assumption of (a) radial dipole orientation or (c) random dipole orientation. The dotted line (b) represents Φ_{ET} values calculated with a pre-averaged orientation factor $\langle|\kappa|\rangle^2 = 0.476$.

for small values of r_1/R_0 is the reduction in the number of acceptors surrounding donors close to the edge of the confining space.

For the case of a cylindrical shell, there are two characteristic length scales to consider. The first is the thickness $(r_1 - r_2)$ of the cylindrical shell, and the second is the radial dimension (r_1) of the cylinder itself. When r_1 is very large, a cylindrical shell will resemble a planar slab. We first consider a cylinder in which we fixed the outer radius at $r_1 = 10R_0$ and varied the inner radius (r_2). As shown in Figure 7, Φ_{ET} increases with the thickness of the shell. This is a restricted geometry effect. At all values of the shell thickness examined, the values of Φ_{ET} for the case of random dipoles (curve (c)) are close to the values obtained assuming $\langle|\kappa|\rangle = 0.6901$. A slight difference was found when $(r_1 - r_2) \leq R_0$. The case of radial dipoles gave higher Φ_{ET} values than random dipoles. The smallest difference in Φ_{ET} values appears at shell thicknesses ranging from R_0 to $2R_0$.

To test whether the results depend on the radial dimension of the cylinder, we carried out a second series of calculations of Φ_{ET} for cylindrical shells with an outer radius of $2R_0$. These

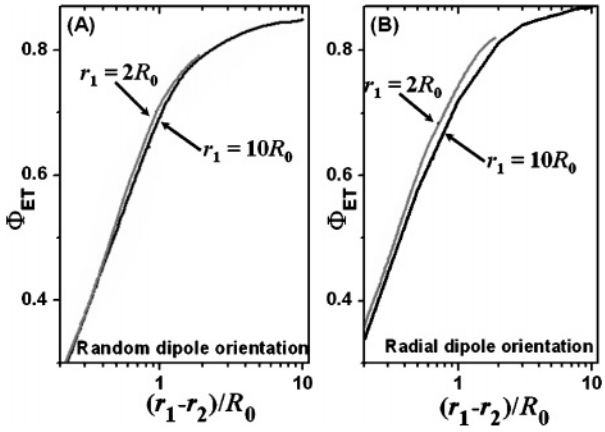

Figure 8. Comparison of Φ_{ET} values as a function with shell thickness calculated for two cylindrical shells with different outer radii: (A) random dipoles; (B) radial dipoles. The details of the calculation are identical to those in Figure 7. The error bars for Φ_{ET} values are omitted for clarity.

values are compared in Figure 8. For the case of random dipoles (Figure 8A), Φ_{ET} is almost independent of the outer radius of the shell. For radial dipoles (Figure 8B), the effect is somewhat larger.

Spherical Geometry. In small spheres and thin spherical shells, there is confinement in the radial direction. As in planar and cylindrical geometries, we introduced donors and acceptors at random, and the number of donors was set at 10 000. For spheres, the choice of acceptor concentration involved a delicate balance of two competing effects. For calculations at $2\pi/3$ acceptors per $4\pi R_0^3/3$ of volume, the number of acceptors was so small that error bars on calculated values were large. For calculations at $8\pi/3$ acceptors per $4\pi R_0^3/3$ of volume, the statistics were improved, but the values of Φ_{ET} were so large that the calculations were not very sensitive to the dimensions of the restricted geometry. In Supporting Information, we provide a plot of Φ_{ET} vs r/R_0 for the higher acceptor concentration. All values of Φ_{ET} are greater than 0.93. One can see that radial dipoles lead to a higher efficiency than that of random dipoles, but these Monte Carlo calculations are not very effective at modeling FRET kinetics in small spherical domains.

The calculations are more effective for spherical shells. In Figure 9, we plot calculated values of Φ_{ET} as a function of the thickness $((r_1 - r_2)/R_0)$ of a spherical shell for an outer radius $r_1 = 10R_0$. Φ_{ET} values are very high for $(r_1 - r_2) > R_0$, but drop rather sharply for thinner shells. This effect is predominantly a restricted geometry effect on the acceptor distribution around each donor. Values of Φ_{ET}, calculated assuming a pre-averaged $\langle|\kappa|\rangle = 0.6901$, are slightly higher than those calculated from pairwise accounting for random dipoles. The rather unrealistic assumption of radial dipole orientation leads to higher values of Φ_{ET} for $(r_1 - r_2) < R_0$. Φ_{ET} values become so close to 1 for thicker shells that it is difficult to assess the consequences of dipole orientation for this case. We also tested whether the results depend on the radial dimension of the sphere. As shown in Figure 10, values of Φ_{ET} for spherical shells with an outer radius $r_1 = 2R_0$ and $r_1 = 10R_0$ are almost independent of the outer radius for the case of random dipoles. A somewhat larger effect is seen for the case of dipoles with a radial orientation.

Confinement Effects on $\langle|\kappa|\rangle$. Monte Carlo simulations of FRET kinetics for random static donors and acceptors confined to a thin planar slice, or to a thin cylindrical or spherical shell, indicate that the use of the pre-averaged orientation parameter

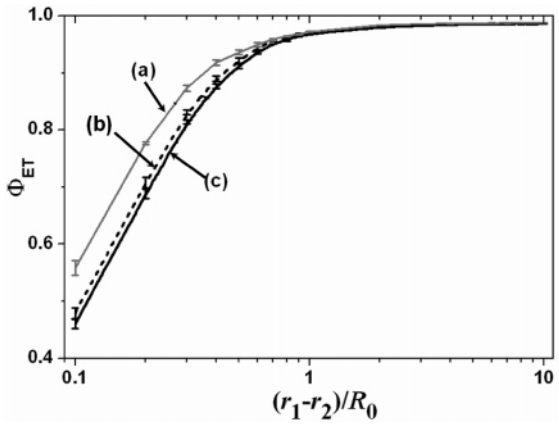

Figure 9. Efficiency of energy transfer Φ_{ET} for randomly distributed donors and acceptors confined to a thin spherical shell as a function of the shell thickness $(r_1 - r_2)/R_0$ for a fixed outer radius ($r_1 = 10R_0$). The acceptor concentration is $8\pi/3$ per $4\pi R_0^3/3$ of volume. (a) Radial dipoles. (c) All dipoles have a random orientation. The dotted line (b) represents Φ_{ET} values calculated using a pre-averaged orientation factor $\langle|\kappa|\rangle^2 = 0.476$.

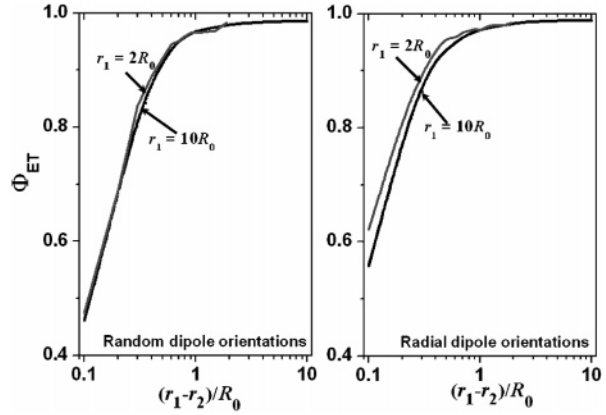

Figure 10. Comparison of Φ_{ET} values as a function with shell thickness calculated for two spherical shells with different outer radii: (A) random dipoles; (B) radial dipoles. The details of the calculation are identical to those in Figure 9. The error bars for Φ_{ET} values are omitted for clarity.

($\langle|\kappa|\rangle^2 = 0.476$) appropriate for uniform 3D space overestimates the magnitude of Φ_{ET} compared to an analysis that takes proper account of the coupling of dipole orientation and D−A separation distance. The effect is small, leading to differences in Φ_{ET} values on the order of only ca. 3% for a confinement dimension of $R_0/2$. As we will see below, the coupling of dipole orientation and separation distance for static random dipoles is more important for the interpretation of donor fluorescence decay profiles. It is useful to note that the correct value of Φ_{ET} in each of these thin-shell geometries can be obtained through the use of a pre-averaged orientation term $\langle|\kappa|\rangle^2 < 0.476$. We present optimum $\langle|\kappa|\rangle^2$ values in Table 2, appropriate for different ratios of the confinement dimension to R_0 for planar objects, as well as cylindrical and spherical shells.

For example, for a thick planar slab, $\langle|\kappa|\rangle^2$ takes the Baumann and Fayer value of 0.476. For $Z = 3R_0$, $\langle|\kappa|\rangle^2 = 0.46$. For $Z = R_0$ and $R_0/2$, $\langle|\kappa|\rangle^2 = 0.42$, and for $Z = R_0/4$, $\langle|\kappa|\rangle^2 = 0.40$. One can see that for these very thin dimensions, the magnitude of the pre-averaged orientation parameter is in the range of 10 to 15% smaller than that for infinite space. The effects are similar for cylindrical or spherical shells. The effect is rather small, and the differences one expects in the quantum efficiencies of energy transfer are within the typical error associated with their experimental determination. These differences, however, are significant for the analysis of experiments in which one tries to interpret donor fluorescence decay profiles in terms of the width of a block copolymer interface.

TABLE 2: Pre-averaged Orientation Factor $\langle|\kappa|\rangle^2$ Suggested for Various Restricted Geometries for the Calculation of FRET Kinetics

planar slab	Z (slab thickness)	$10R_0$	$3R_0$	R_0	$0.5R_0$	$0.25R_0$
	$\langle|\kappa|\rangle^2$	0.47	0.46	0.42	0.42	0.40
		r_1-r_2 (shell thickness)				
	r_1 (outer radius)	$10R_0$	$3R_0$	R_0	$0.5R_0$	$0.25R_0$
cylindrical shell	$10R_0$	0.47	0.46	0.42	0.41	0.40
	R_0			0.41	0.42	0.42
spherical shell	$10R_0$	0.47	0.46	0.43	0.40	0.40
	R_0			0.42	0.37	0.37

Determining the Interface Thickness of a PI−PMMA Lamella. In this section, we reanalyze donor fluorescence decay profiles for samples of donor- and acceptor-labeled PI−PMMA reported in ref 1. Experimental data were obtained for a series of samples containing mixtures of the Phe- (donor) and An- (acceptor) labeled polymers of similar chain length and composition. Each sample was annealed at 130 °C for 5 h. SAXS measurements of the lamellar spacing and $I_D(t)$ decay profiles were measured on samples cooled to room temperature. Theoretical donor decay profiles generated through the use of eqs 8 or 9 are "noise-free" and correspond to instantaneous sample excitation. Experimental decay profiles contain Poisson noise associated with the single-photon timing measurement technique as well as an instrument response function. To analyze experimental data, theoretical decay profiles calculated from the simulated data were first convoluted with the instrument response function ("lamp profile") of the actual experiment. Using the interface thickness as a variable parameter, a series of theoretical decay profiles were constructed for each sample of different acceptor content, and then compared with the experimental decay profile of the appropriate sample to obtain the best fit for each sample.

Examples of the best-fit results for three different sample compositions are shown in Figure 11. These fits were generated with theoretical donor decay profiles calculated via eq 8 for static random dipoles, in which the width of the interface and the concentration of acceptors as described by eqs 10 and 11 determine the distribution of r_{jk} values. For each acceptor concentration, the value of interface thickness corresponding to the best fit of the experimental decay (minimum on the χ^2 surface) is the optimized value of interface thickness. We average the best-fit values of the interface thickness to obtain a value of $\delta = 0.9 \pm 0.2$ nm (Table 3).

In ref 1, we reported a value of $\delta = 1.3 \pm 0.2$ nm for these samples. To obtain this value, the same experimental $I_D(t)$ profiles were compared with theoretical profiles generated through the use of eqs 3 and 10, using $\langle|\kappa|\rangle^2 = 0.476$. To identify the origin of this difference, we take advantage of our finding that, for D and A confined to thin rectangular solids, FRET data can be analyzed using a pre-averaged orientation parameter somewhat smaller than that appropriate for homogeneous 3D space. For the Phe- and An-labeled PI−PMMA sample under consideration, $R_0 = 2.3$ nm and $\delta \approx 1$ nm, corresponding to a confinement length scale of $Z \approx 0.4\ R_0$. From the data in Table 2, we estimate an appropriate value for a pre-averaged orientation parameter of $\langle|\kappa|\rangle^2 = 0.41$. Repeating the calculation of the theoretical decay profiles with eq 9 using this value for $\langle|\kappa|\rangle^2$, we obtain $\delta = 1.0 \pm 0.1$ nm. As a check on the data analysis strategy, we also generated theoretical decay profiles using eq

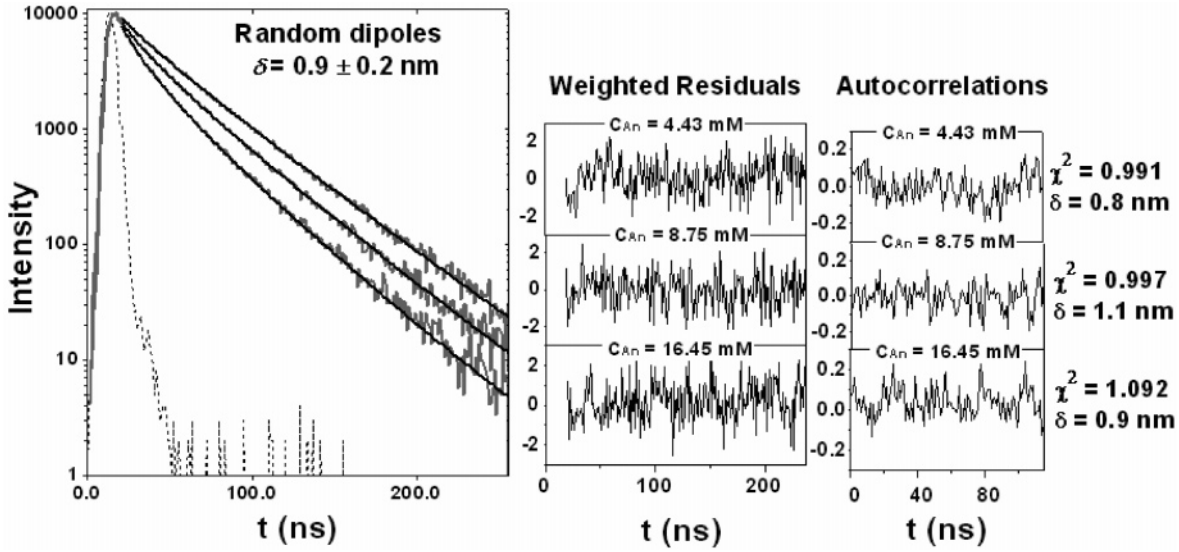

Figure 11. Left figure: donor fluorescence decays (from ref 1) from films of PI-9Phe-PMMA + PI-2An-PMMA copolymer mixtures (from top to bottom: samples 1 to 3, listed in Table 1) annealed at 130 °C for 5 h. The dotted line is the instrument response function, obtained by exciting a solution of *p*-terphenyl in deaerated cyclohexane (lifetime: 0.96 ns). Each black solid line is the best fit of the fluorescence decay, calculated using eq 8 and the dye loci generated by Monte Carlo calculations for the corresponding model system. The optimized interface thickness was recovered from those best fits. Right figures: weighted residuals and the autocorrelation of the weighted residuals for the best fits. Values of χ^2 for the nonlinear least-squares fit and the optimized interface thickness for each An concentration are indicated at the right side of the figure. The values of the An concentration **(**C_A^0) are indicated in each figure. All dipoles were assumed to have a random orientation. In all calculations, we considered the individual orientation factor for each D−A pair. The average interface thickness for all samples (0.9 ± 0.2 nm) is also shown in the figure.

TABLE 3: Optimized Value of Interface Thickness for PI-9Phe-PMMA/PI-2An-PMMA Samples Annealed for 5 h at 130 °C

method	Monte Carlo			eq 3	
$\langle\|\kappa\|\rangle^2$	0.476	0.41	random dipoles	0.476	0.41
δ (nm)	1.3 ± 0.3	1.0 ± 0.1	0.9 ± 0.2	1.3 ± 0.2	1.0 ± 0.2

3 in conjunction with $\langle|\kappa|\rangle^2 = 0.41$. Here, we obtain $\delta = 1.0 \pm 0.2$ nm. We can conclude that the wider interface deduced in ref 1 was a consequence of neglect of the coupling of dipole orientation and D−A separation in the very narrow interface between PI and PMMA in these block copolymer lamellae. Proper accounting for the orientation parameter leads to about a 30% reduction in the fitted value of the interface thickness.

To put these results in perspective, one should note that PI and PMMA are strongly immiscible polymers. The width of the interface that we report here is the smallest ever determined for a block copolymer. For a different block copolymer, poly(styrene-*b*-methyl methacrylate) (PS−PMMA), the width of the interface is larger, ca. 5 nm. For FRET experiments on lamellar samples of this block copolymer using the same Phe/An donor−acceptor pair, the confinement scale is greater than $2R_0$. From the data in Table 2, we can infer that, in the analysis of FRET data on these samples, the error associated with assuming $\langle|\kappa|\rangle^2 = 0.476$ is very small.

Summary

In this paper, we described the use of a Monte Carlo methodology to study FRET in restricted geometries. We first examined Euclidean spaces in which the restricted geometry was a thin planar slab, a thin cylinder or cylindrical shell, or a thin spherical shell to investigate the magnitude of the coupling of the orientation parameter with the donor−acceptor separation. One expects this coupling to become increasingly important as the mean D−A separation decreases. For geometries that are large with respect to R_0, the pre-averaged orientation parameter derived by Baumann and Fayer ($\langle|\kappa|\rangle^2 = 0.476$ for 3D) can be used. To investigate whether one could continue to employ this pre-averaged value for the case of restricted geometries, we compared values of the energy transfer efficiency Φ_{ET} calculated pairwise with proper consideration of the dipole orientation with that calculated using the Baumann and Fayer value for 3D space. For random dipole orientation, the differences were very small. There were vestiges in each calculation of the coupling of dipole orientation and distance expected for nonradiative energy transfer. Values of Φ_{ET} calculated with the pre-averaged value were always higher than those obtained by proper consideration of the coupling of orientation and distance. The "correct" value Φ_{ET} for very small domains could be reproduced using a pre-averaged value of the orientation parameter somewhat smaller than that appropriate for homogeneous 3D space. These values are presented in Table 2.

The coupling between dipole orientation and D−A distance leads to a nonnegligible effect when we used the FRET methodology to determine the interface thickness for PI−PMMA block copolymer lamellae. In these polymers, the donor and acceptor dyes were covalently attached to the junction between the PI and PMMA blocks. The value of interface thickness retrieved from FRET method by considering individual dipole orientations was found to be 0.9 ± 0.2 nm. Results published previously yielded a larger value (1.3 ± 0.2 nm) of the interface width. This value was obtained through a data analysis method that assumed a pre-averaged orientation factor $\langle|\kappa|\rangle^2 = 0.476$. This larger interface thickness value originates from neglect of the coupling of dipole orientation and D−A distance when the dyes are confined to a very narrow lamellar interface. Our results for planar-slab-restricted geometries suggest that one can carry out a reasonable calculation of the interface width from FRET data by employing a pre-averaged orientation term slightly smaller than the value appropriate for homogeneous 3D space. If we use a modified pre-averaged orientation factor appropriate for planar slices ca. 1 nm thick, we obtain a value of 1.0 ± 0.2 nm for the thickness of PI−PMMA lamellar interface. This value is in good accord with the value obtained through the

Monte Carlo methodology that takes proper account of the coupling of dipole orientation and D−A separation distance in the analysis of experimental FRET data.

Acknowledgment. We thank NSERC Canada and the ORDCF program of the Province of Ontario for their support of this research.

Supporting Information Available: A plot of the efficiency of energy transfer vs radius for D and A dyes confined to a sphere. This material is available free of charge via the Internet at http://pubs.acs.org.

References and Notes

(1) Yang, J.; Roller, S. R.; Winnik, M. A.; Zhang Y.; Pakula, T. *Macromolecules* **2005**, *38*, 1256.
(2) Winnik M. A., Ed. *Photophysical and Photochemical Tools in Polymer Science*; D. Reidel: Dordrecht, The Netherlands, 1985.
(3) Föster, T. *Naturwissenschaften* **1946**, *6*, 166.
(4) Wu, P.; Brand, L. *Biochemistry* **1992**, *31*, 7939.
(5) Klafter, J.; Blumen, A. *J. Chem. Phys.* **1984**, *80*, 874.
(6) Klafter, J.; Drake, J. M. *Molecular Dynamics in Restricted Geometries*; Wiley: New York, 1989.
(7) Drake, J. M.; Klafter, J.; Levitz, P. *Science* **1991**, *251*, 1574.
(8) Yekta, A.; Duhamel, J.; Winnik. M. A. *Chem. Phys. Lett.* **1995**, *235*, 119.
(9) Farinha, J. P. S.; Spiro, J. G.; Winnik, M. A. *J. Phys. Chem. B* **2004**, *108*, 16392.
(10) Ni, S.; Zhang, P.; Wang Y.; Winnik, M. A. *Macromolecules* **1994**, *27*, 5742.
(11) Tcherkasskaya, O.; Ni, S.; Winnik, M. A. *Macromolecules* **1996**, *29*, 4241.
(12) Rharbi, Y.; Winnik, W. A. *Macromolecules* **2001**, *34*, 5238.
(13) Yang, J.; Lu, J.; Rharbi, Y.; Cao L.; Winnik M. A.; Zhang, Y.; Weisner, U. *Macromolecules* **2003**, *36*, 4485.
(14) Helfand, E.; Tagami, Y. *J. Chem. Phys.* **1972**, *56*, 3592; Helfand, E.; Wasserman, Z. R. *Macromolecules* **1980**, *13*, 994.
(15) Semenov, A. N. *Sov. Phys. JETP* **1985**, *61*, 733.
(16) Matsen, M. W.; Schick, M. *Phys. Rev. Lett.* **1994**, *72*, 2660.
(17) Snyder, B.; Freire, E. *Biophys. J.* **1982**, *40*, 137.
(18) Freire, E.; Snyder, B. *Biochim. Biophys. Acta* **1980**, *600*, 643.
(19) Frederix, P. L. T. M.; de Beer, E. L.; Hamelink, W.; Gerritsen, H. C. *J. Phys. Chem. B* **2002**, *106*, 6793.
(20) Bagchi, B.; Srinivas, G. *J. Phys. Chem. B* **2001**, *105*, 9370.
(21) Uhlik, F.; Limpouchová, Z.; Matějíček, P.; Procházka, K.; Tuzar, Z.; Webber, S. E. *Macromolecules* **2002**, *35*, 9497.
(22) Yang, J.; Winnik, M. A.; Pakula, T. *Macromolecules*, **2005**, in press.
(23) Baumann, J.; Fayer, M. D. *J. Chem. Phys.* **1986**, *85*, 4087.
(24) Helfand, E. *Macromolecules* **1975**, *8*, 552.
(25) Bennett, R. G. *J. Chem. Phys.* **1964**, *41*, 3037.